Electronic Supplementary Information

Greatly enhanced ultrafast optical absorption nonlinearities of pyridyl perovskite nanocrystals axially modified by star-shaped porphyrins

*Zihao Guan[†a], Lulu Fu[†a], Lu Chen[†], Zhiyuan Wei[†], Fang Liu[†], Yang Zhao[†], Zhipeng Huang[†], Mark G. Humphrey[‡], and Chi Zhang[†]**

[†] China-Australia Joint Research Center for Functional Molecular Materials, School of Chemical Science and Engineering, Tongji University, Shanghai 200092, China.

[‡] Research School of Chemistry, Australian National University, Canberra, ACT 2601, Australia.

* Corresponding author. E-mail: chizhang@tongji.edu.cn (Chi Zhang).

[a] These authors contributed equally.

1. Experimental Procedures

The synthesis of compounds **1** and **2** can be prepared with reference to reported literature.[1,2] The preparation procedures of compounds dipyrromethane and 1,5-dihexyloxy benzaldehyde referred to the reported literature using two- or three-step synthesis methods,[3,4] and the specific synthetic steps of other compounds are as follows:

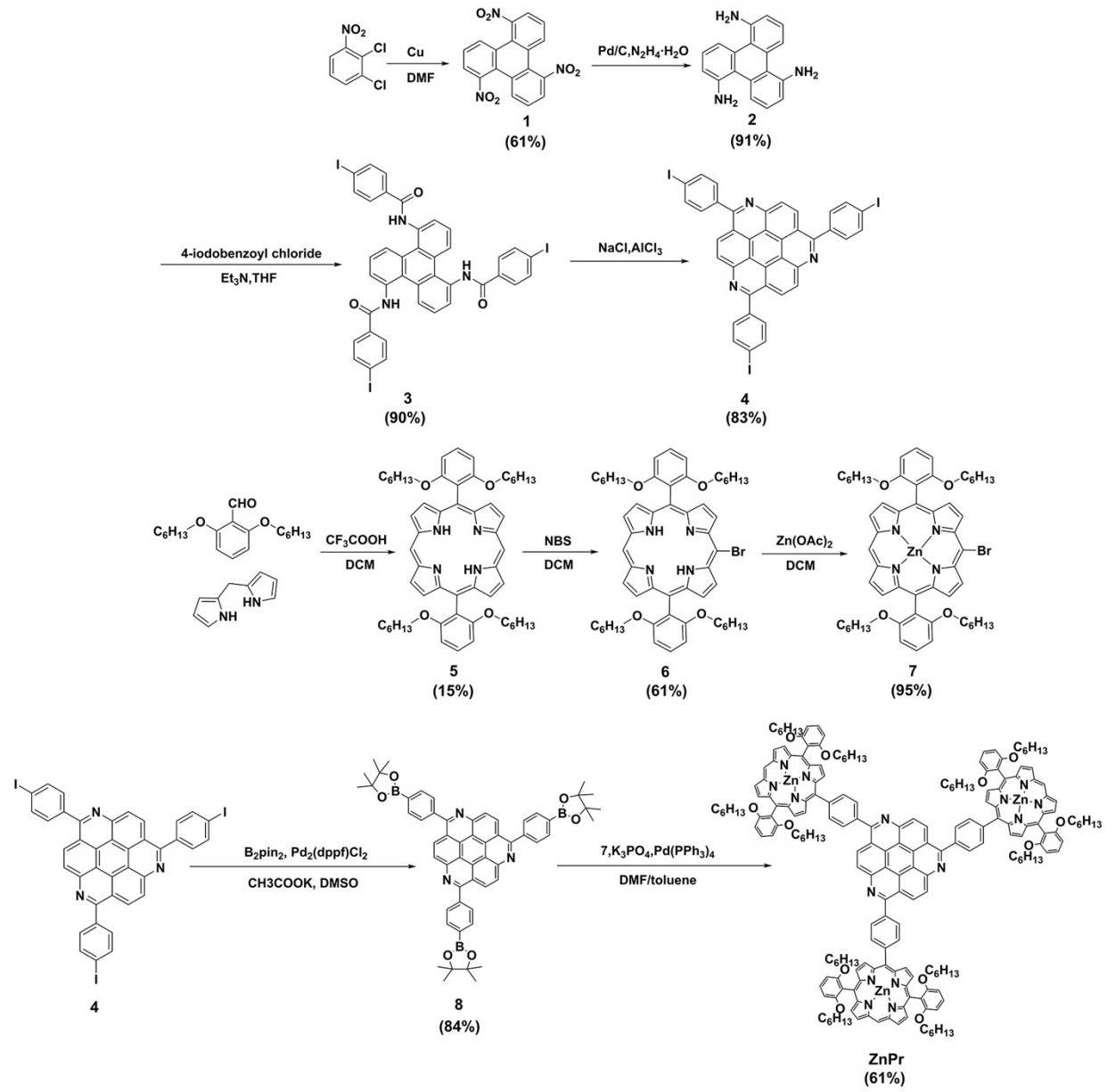

Scheme S1. The synthetic route of target porphyrin ZnPr.

1.1. *N,N′,N″*-(Triphenylene-1,5,9-triyl)tris(4-iodobenzamide) (3)

To a solution of **2** (0.15 g, 0.56 mmol) in anhydrous tetrahydrofuran (THF) (5 mL) with Et_3N (0.33 g, 3.3 mmol) was added dropwise 4-iodobenzoyl chloride (0.66 g, 2.5 mmol) dissolved in anhydrous THF (3 mL). The mixture was stirred at room temperature under nitrogen atmosphere for overnight.

After the reaction was completed, To the reaction was added dichloromethane and saturated $NaHCO_3$ solution and the mixture was stirred for 5 min. The mixture was extracted with CH_2Cl_2, the organic layer was separated and the aqueous phase was extracted with CH_2Cl_2. The combined organic phase was washed with saturated $NaCO_3$ solution, water, brine respectively and dried over Na_2SO_4. After filtration, the filter was dried in vacuum to give the crude product which was purified by washing with CH_2Cl_2 affording the pure product **3** as a white solid. Yield: 0.49 g (90%);^{1}H NMR (600 MHz, DMSO-d_6, δ): 10.79 (s, 3H), 7.97 (d, J = 8.0 Hz, 6H), 7.83 (d, J = 8.0 Hz, 6H), 7.50 (d, J = 7.6 Hz, 3H), 7.41 (t, J = 7.9 Hz, 3H).

1.2. 2,6,10-Tri(4-iodophenyl)-1,5,9-triazocoronene (4)

Compound **3** (68 mg, 0.07 mmol), sodium chloride (204 mg, 3.5 mmol), and anhydrous aluminum chloride (160 mg, 1.2 mmol) were charged into a two-necked flask under nitrogen atmosphere. The mixture was stirred at 220 ℃ for 5 h. After cooled to room temperature, the mixture was basified with 20% aqueous NaOH solution and filtered, the filter washed with water and dried to give crude product which dispersed ultrasonically in mixture solution of CH_2Cl_2/MeOH = 10:1, and filtered. The filtrate was washed with hot CH_2Cl_2 or CH_2Cl_2/MeOH and dried in vacuum to afford the pure product **4** as a yellow solid. Yield: 53 mg (83%) ^{1}H NMR (600 MHz, $CHCl_3$-d, δ): 9.22 (d, J = 9.5 Hz, 1H), 9.16 (d, J = 8.9 Hz, 1H), 8.13 (d, J = 7.9 Hz, 1H), 7.94 (d, J = 7.7 Hz, 1H).

1.3. 5,15-Bis(2,6-bis(hexyloxy)phenyl)porphyrin (5)

To a degassed solution of dipyrromethane (6.05 g, 41.4 mmol) and 1,5-dihexyloxy benzaldehyde (12.7 g, 41.4 mmol) in CH_2Cl_2 (5.4 L) was added trifluoroacetic acid (2.75 mL, 37.3 mmol). After the solution was stirred at 23 °C under N_2 for 4 h, 2,3-dichloro-5,6-dicyano-1,4-benzoquinone (14.1 g, 62.1 mmol) was added and the mixture was stirred for an additional 1 h. The mixture was quenched with Et_3N (7 mL), filtered through silica and dried over anhydrous Na_2SO_4. The solvent was removed by rotary evaporation. The residue was purified by column chromatography (silica gel, DCM:PE = 1:2) to give **5** as a purple powder. Yield: 2.68 g (15%). ^{1}H NMR (600 MHz, $CHCl_3$-d, δ): 10.14 (s, 2H), 9.26 (d, J = 4.4 Hz, 4H), 8.97 (d, J = 4.4 Hz, 4H), 7.70 (t, J = 8.5 Hz, 2H), 7.02 (d, J = 8.6 Hz, 4H), 3.83 (t, J = 6.4 Hz, 8H), 0.90 (m, 8H), 0.51 (m, 16H), 0.41 (m, 8H), 0.26 – 0.21 (m, 12H), −3.02 (s, 2H).

1.4. 5,15-bis(2,6-bis(hexyloxy)phenyl)-10-bromoporphyrin (6)

Porphyrin **5** (310 mg, 0.36 mmol) was dissolved in CH_2Cl_2 (150 mL) under N_2. The solution was

cooled to 0 ℃, and then a solution of *N*-bromosuccinimide (67 mg, 0.38 mmol) in CH_2Cl_2 (40 mL) was added and stirred for 4h at 0 °C under N_2. After the reaction was quenched with acetone (5 mL), filtered through silica and dried over anhydrous Na_2SO_4. The solvent was removed by rotary evaporation. The residue was purified by column chromatography (silica gel, CH_2Cl_2:petroleum ether = 1:3) and recrystallized from MeOH/CH_2Cl_2 to give **6** (2.3 g, 61%) as a purple powder. Yield: 0.21 g (61%). ^{1}H NMR (600 MHz, $CHCl_3$-*d*, δ): 10.01 (s, 1H), 9.62 (d, *J* = 4.6 Hz, 2H), 9.17 (d, *J* = 4.3 Hz, 2H), 8.88 (t, *J* = 5.1 Hz, 4H), 7.70 (t, *J* = 8.5 Hz, 2H), 7.00 (d, *J* = 8.6 Hz, 4H), 3.83 (t, *J* = 6.3 Hz, 8H), 0.94 – 0.90 (m, 8H), 0.53 – 0.49 (m, 16H), 0.41 – 0.38 (m, 8H), 0.23 (t, *J* = 6.8 Hz, 12H), −2.88 (s, 2H).

1.5. Zn(II) 5-Bromo-10,20-bis(2,6-bis-hexyloxyphenyl)porphyrin (7)

To a mixture of porphyrin **6** (0.94 g, 1 mmol) and $Zn(OAc)_2$•$2H_2O$ (2.2 g, 10 mmol) in a mixture of CH_2Cl_2 (200 mL) and MeOH (100 mL) was stirred at room temperature for 4 h. After the reaction was quenched with water (100 mL), and the mixture was extracted with CH_2Cl_2 (2 × 100 mL) and separated. The combined extracts were washed with water and dried over anhydrous Na_2SO_4. The solvent was removed by rotary evaporation. The residue was purified by column chromatography (silica gel, CH_2Cl_2:petroleum ether = 1:3) and recrystallized from MeOH/CH_2Cl_2 to give **7** as a purple powder. Yield: 0.96 g (95%).^{1}H NMR (600 MHz, $CHCl_3$-*d*, δ): 10.01 (s, 1H), 9.62 (d, *J* = 4.6 Hz, 2H), 9.17 (d, *J* = 4.3 Hz, 2H), 8.88 (t, *J* = 5.1 Hz, 4H), 7.70 (t, *J* = 8.5 Hz, 2H), 7.00 (d, *J* = 8.6 Hz, 4H), 3.83 (t, *J* = 6.3 Hz, 8H), 0.94 – 0.90 (m, 8H), 0.53 – 0.49 (m, 16H), 0.41 – 0.38 (m, 8H), 0.23 (t, *J* = 6.8 Hz, 12H).

1.6. 2,6,10-Tri(pinacyl phenylborate)-1,5,9-triazocoronene (8)

A mixture of compound **4** (0.64 g, 0.7 mmol), $Pd_2(dppf)Cl_2$ (73 mg, 0.1 mmol), and CH_3COOK (0.41 g. 4.2 mmol) in dry dimethyl sulfoxide (DMSO, 40 mL) was degassed by bubbling N_2 for 1h, and the mixture was heated up to 80℃ then bis(pinacolato)diboron (1.07 g, 4.2 mmol) was added and stirred for 12 h at 75℃ at under N_2. After the reaction was completed, the reaction solvent was removed under reduced pressure and the residue was dissolved in CH_2Cl_2. The solution was washed with brine and water many times, dried over anhydrous Na_2SO_4, and the solvent was removed by rotary evaporation. The residue was purified by column chromatography (silica gel, EtOAc:petroleum ether = 1:2) to give **10** as a faint yellow solid. Yield: 0.53 g (84%).^{1}H NMR (600 MHz, $CHCl_3$-*d*, δ): 9.19 (d, *J* = 8.8 Hz, 3H), 9.12 (d, *J* = 8.8 Hz, 3H), 8.20 (q, *J* = 7.2 Hz, 12H), 1.46 (d, *J* = 1.8 Hz, 36H).

1.7. 2,6,10-Tri(4-(10,20-bis(2,6-bis(hexyloxy)phenyl)zincporphyrinylacetenyl) phenyl)-1,5,9-triazocoronene (ZnPr)

ZnPr was synthesized on the basis of the Suzuki-Miyaura coupling reaction, which is a palladium-catalyzed cross-coupling reaction of organoboranes with organic halides in the presence of a base (transmetallation is reluctant to occur without the activating effect of a base).[5] Specifically, a mixture of compound **8** (55 mg, 0.06 mmol), porphyrin **7** (332 mg, 0.34 mmol), K_3PO_4 (60 mg, 0.358 mmol), and tetrakis(triphenylphosphine)palladium(0) (70 mg, 0.06 mmol) in anhydrous *N*,*N*-dimethylformamide (DMF, 30 mL) and toluene (14 mL) was degassed by bubbling N_2 for 30 min and heated at 90°C for 12 h under N_2. After removal of insoluble materials by filtration through a celite, the filtrate was treated with CH_2Cl_2 and washed with saturated Na_2CO_3 solution, water, brine respectively. After dried over Na_2SO_4, the solvent was evaporated to give the residue which was purified by flash silica gel chromatography eluting with petroleum ether/CH_2Cl_2/THF (2:1:0.1) and recrystallized from CH_3OH/CH_2Cl_2 to afford **ZnPr** as a purple powder. Yield: 121 mg (61%).^{1}H NMR (600 MHz, $CHCl_3$-*d*, δ): 10.17 (s, 3H), 9.89 (d, *J* = 8.6 Hz, 3H), 9.64 (d, *J* = 8.6 Hz, 3H), 9.35 (d, *J* = 4.2 Hz, 6H), 9.24 (d, *J* = 4.4 Hz, 6H), 9.08 (d, *J* = 4.3 Hz, 12H), 8.69 (d, *J* = 9.2 Hz, 12H), 7.74 (t, *J* = 8.6 Hz, 6H), 7.06 (d, *J* = 8.7 Hz, 12H), 3.89 (t, *J* = 6.3 Hz, 24H), 1.01 – 0.84 (m, 30H), 0.54 – 0.45 (m, 42H), 0.40 – 0.36 (m, 24H), 0.24 (t, *J* = 6.9 Hz, 36H).^{13}C NMR (151 MHz, $CHCl_3$-*d*, δ): 162.61, 160.22, 150.82, 150.75, 149.66, 149.40, 145.25, 144.80, 138.47, 135.17, 131.89, 131.61, 131.43, 129.80, 129.43, 129.22, 129.08, 126.87, 123.54, 121.68, 121.44, 119.10, 115.74, 113.08, 105.52, 104.92, 68.78, 30.89, 28.68, 24.93, 22.07, 13.57. HRMS (MALDI-TOF) *m/z*: $[M]^+$ calcd. for $C_{213}H_{219}N_{15}O_{12}Zn_3$, 3305.26; found, 3304.82.

2. Transient Absorption (TA) Measurements

Fs TA spectroscopy measurements of perovskite NC films, were performed using our custom-built TA setup. The light pulse generated by the Spectra-Physics Spirit laser (350 fs, 1 kHz) is split into two parts by an ultrafast beam splitter with a reflection to transmission energy ratio of 1:4. A frequency-doubled 520 nm output from the transmitted light was used as the pump beam, whereas the reflected laser pulse was used to excite a sapphire crystal for generating white light continuous (WLC) spectrum, whose chirp effect is corrected. The pump beam was chopped at 500 Hz, and the probe beam transmitting the sample was collected by an ultrafast fiber optic spectrometer after passing through a short pass filter with a cutoff wavelength of 950 nm. The pump light and probe light overlap at the

same point of the sample in a noncollinear manner. All measurements are carried out at room temperature (20 ℃).

3. Two-photon PL measurements

The Two-photon PL excitation beam was generated by a regeneratively amplified Ti:sapphire laser system (Coherent Chameleon, 100 fs, 800 nm, 80 MHz). The two-photon PL signal is collected at the right angles from excited perovskite NC film. The signal is guided into the spectrometer (Spectr Pro 500i PI Acton) through a fiber. Finally, it is detected by an intensified charge coupled device (ICCD, PIMAX4, Princeton Instruments).

4. Temperature-dependent PL measurements

Variable temperature PL spectra of perovskite NCs were also collected using an Edinburgh Instruments FLS980 steady-state/transient fluorescence spectrometer. The temperature-dependent integrated PL intensity (I) of perovskite NCs was fitted using Formula S1.

$$I = \frac{I_0}{1 + A\exp(-\frac{E_b}{k_B T})} \quad \text{(S1)}$$

Here, I_0 represents the integrated PL intensity at 0 K, A is the radiative decay constant, E_b is the binding energy of excitons, and k_B is the Boltzmann constant with a value of approximately 0.086186 meV/K.

5. Calculation of nonlinear absorption parameters in SA

The SA process of our perovskite NC materials can be reasonably analyzed through the Frantz-Nodvik equation, and the corresponding ground state and excited state absorption cross-section values can be obtained. The mathematical model formula is as follows.[6-8]

$$T = T_0 + \frac{T_{FN} - T_0}{1 - T_0}(T_1 - T_0) \quad \text{(S2)}$$

$$T_0 = e^{-N\sigma_g L} \quad \text{(S3)}$$

$$T_1 = e^{-N\sigma_e L} \quad \text{(S4)}$$

$$T_{FN} = \frac{\ln\left(1 + T_0\left[e^{\sigma_{g2}\frac{E}{}} - 1\right]\right)}{\sigma_g \frac{E}{2}} \quad \text{(S5)}$$

Here T represents the normalized transmittance, T_0 denotes the linear transmittance, T_1 corresponds to the maximal transmittance that can be achieved at very high pulse fluence. The term N refers to the absorber density, defined as the number of absorbing entities per unit volume; in this case, it represents the molar density of $CsPbBr_3$. The parameters σ_g and σ_e are the GSA and ESA cross sections, respectively, while L denotes the sample thickness. T_{FN} describes the transmission of an "ideal" saturable absorber (where $\sigma_e \equiv 0$), and E represents the input beam fluence in units of photons per unit area.

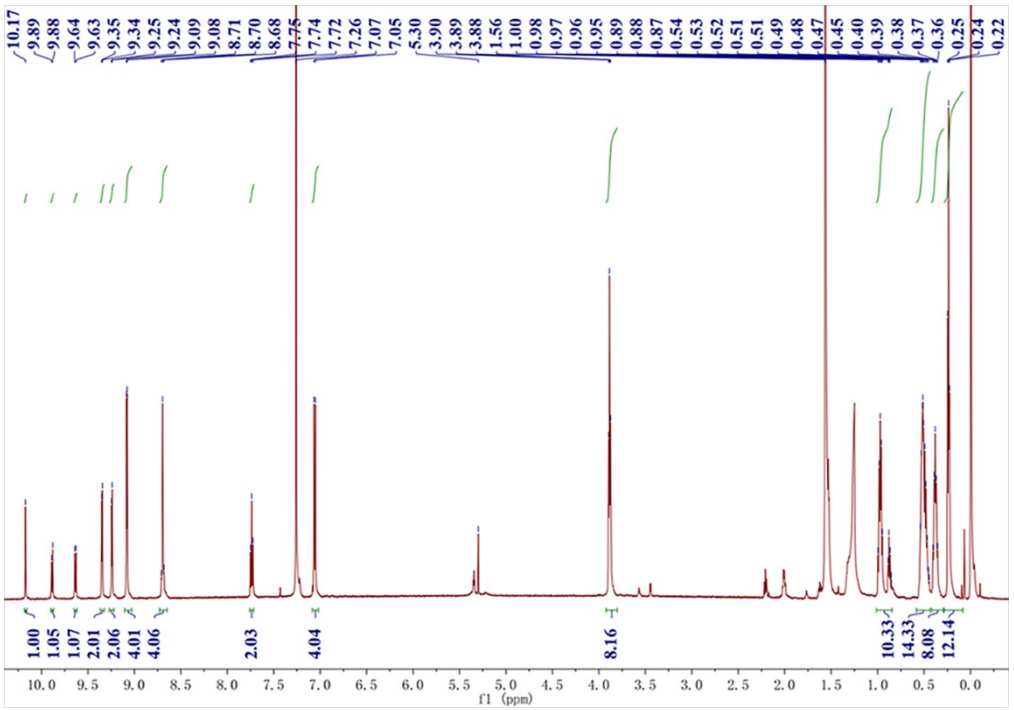

Figure S1. ^{1}H NMR spectrum of ZnPr.

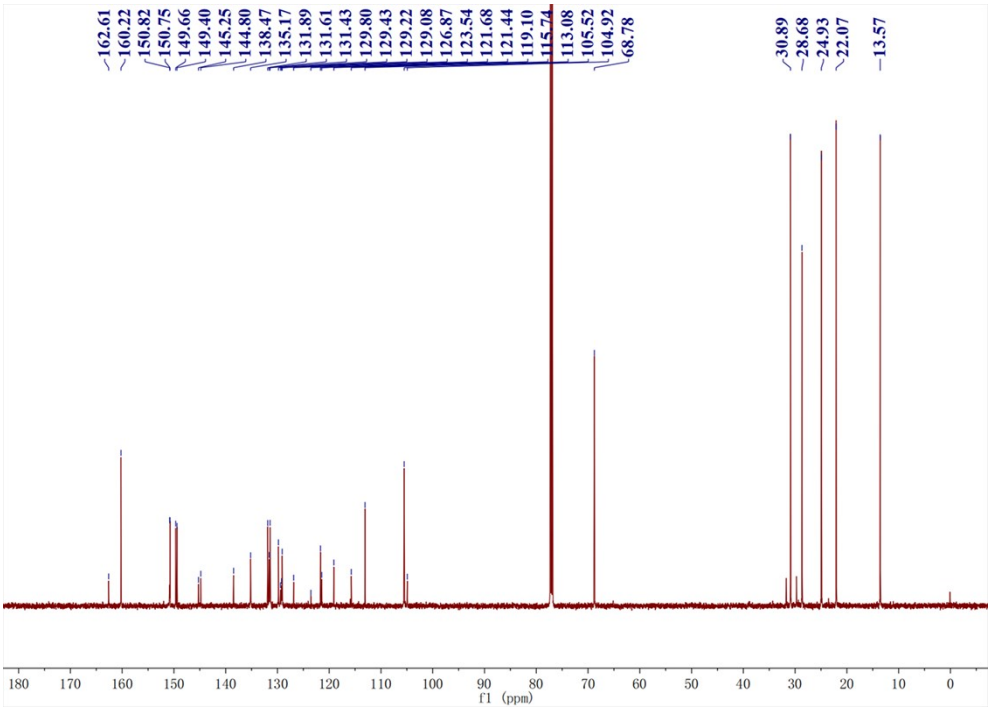

Figure S2. ^{13}C NMR spectrum of ZnPr.

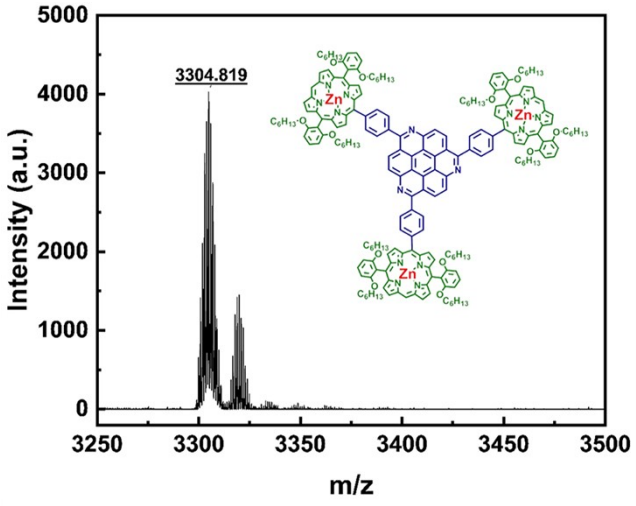

Figure S3. MALDI-TOF spectrum of ZnPr.

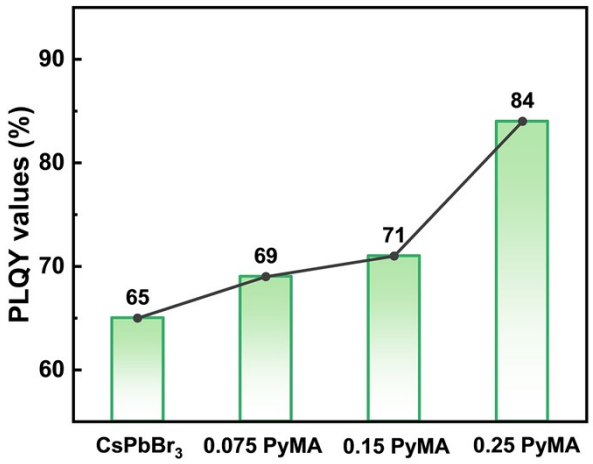

Figure S4. PLQY values for $CsPbBr_3$ NCs without and with different contents of PyMA treatment. "0.075, 0.15, and 0.25 PyMA" represent "0.075, 0.15, and 0.25 PyMA-$CsPbBr_3$-NC".

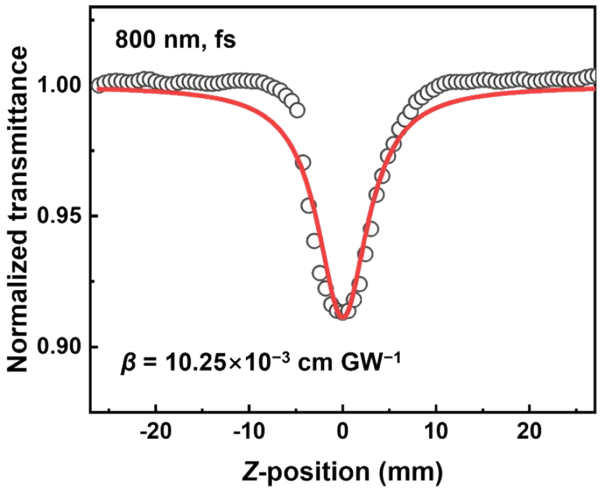

Figure S5. Open-aperture Z-scan of ZnPr monomer under 800 nm fs laser excitation.

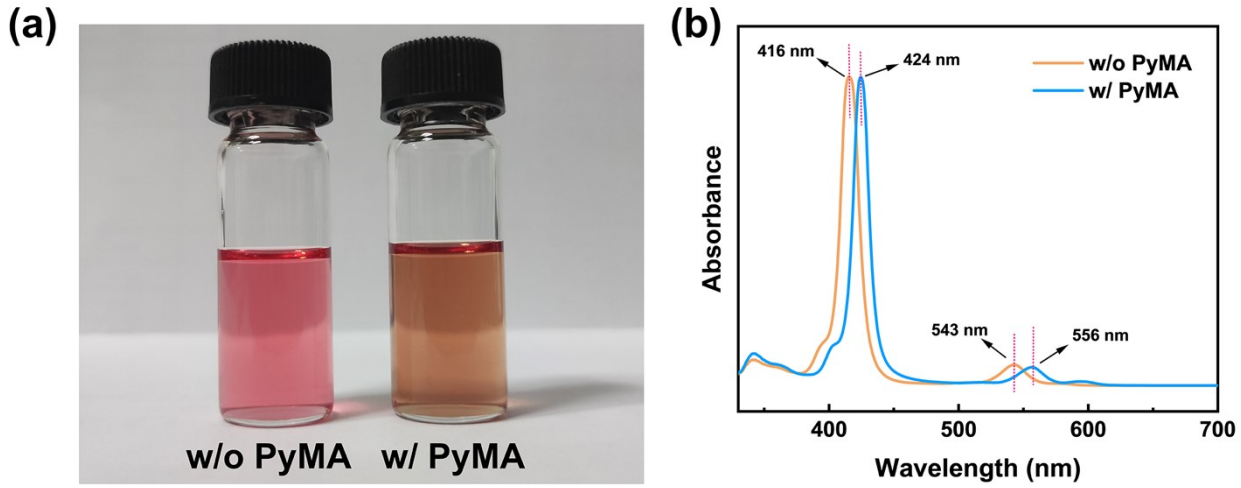

Figure S6. (a) Photograph and (b) UV−vis absorption spectra for ZnPr dissolved in the CH_2Cl_2

solution without (w/o) and with (w/) PyMA.

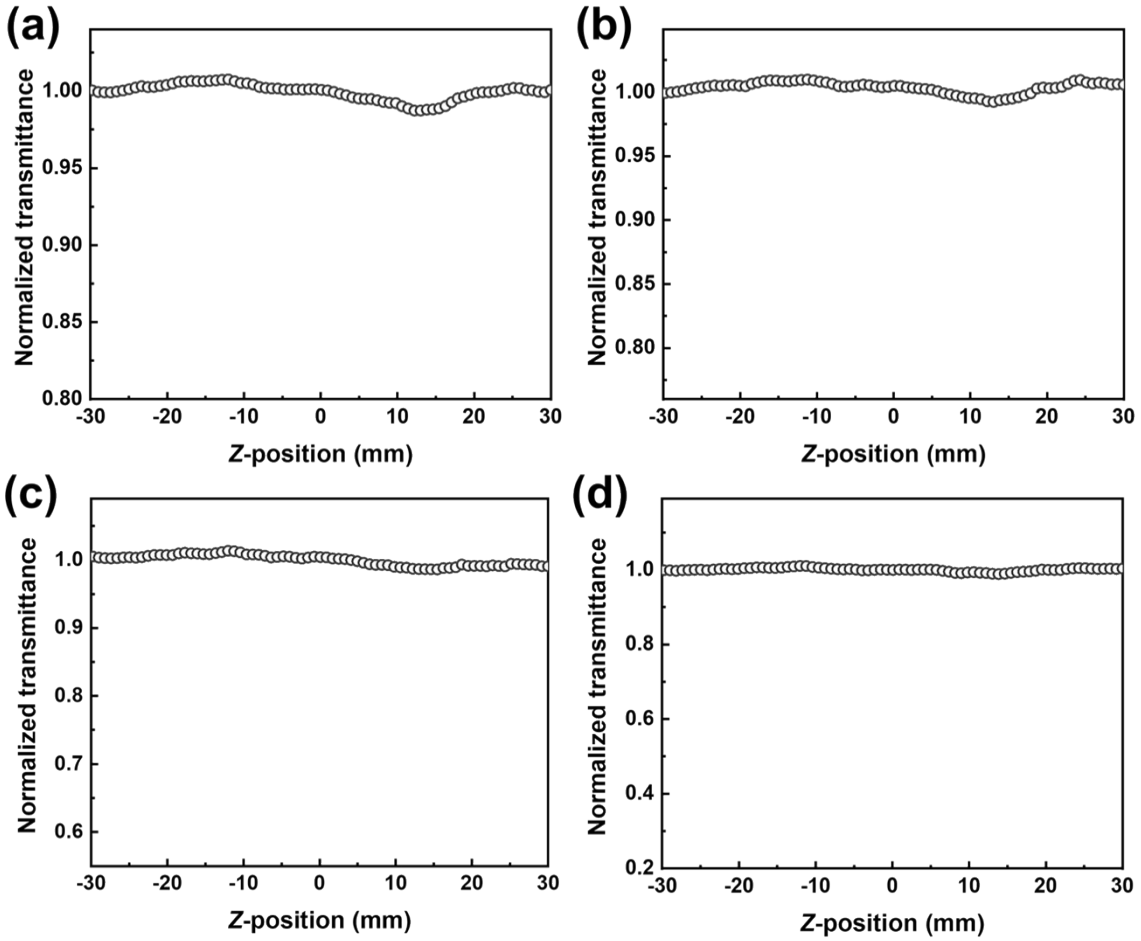

Figure S7 Open-aperture Z-scan curves of the PMMA substrate under the fs laser at 800 nm with different pulse energies of (a) 56 nJ, (b) 78 nJ, (c) 146 nJ, (d) 205 nJ.

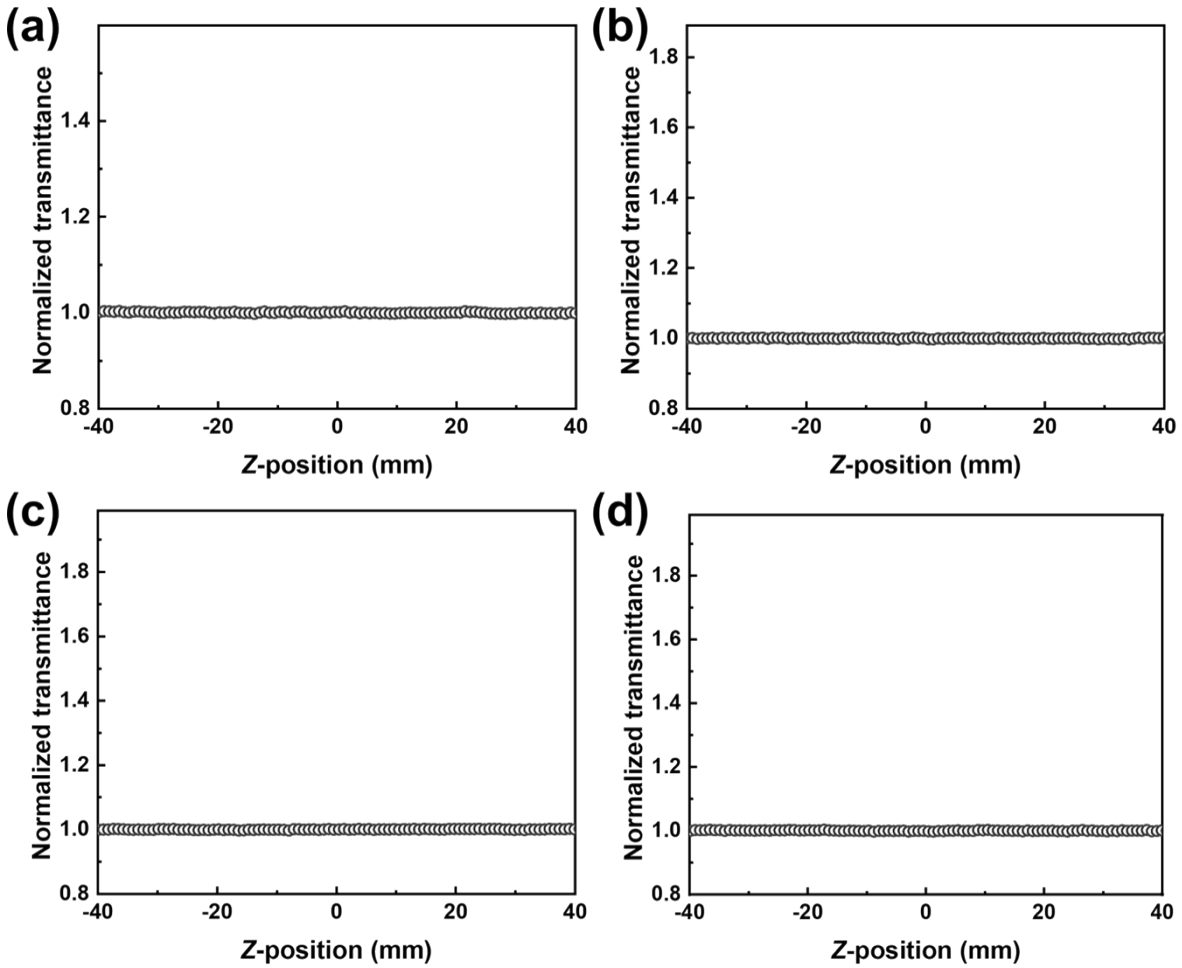

Figure S8. Open-aperture Z-scan curves of the PMMA substrate under the fs laser at 515 nm with different pulse energies of (a) 175 nJ, (b) 290 nJ, (c) 346 nJ, (d) 400 nJ.

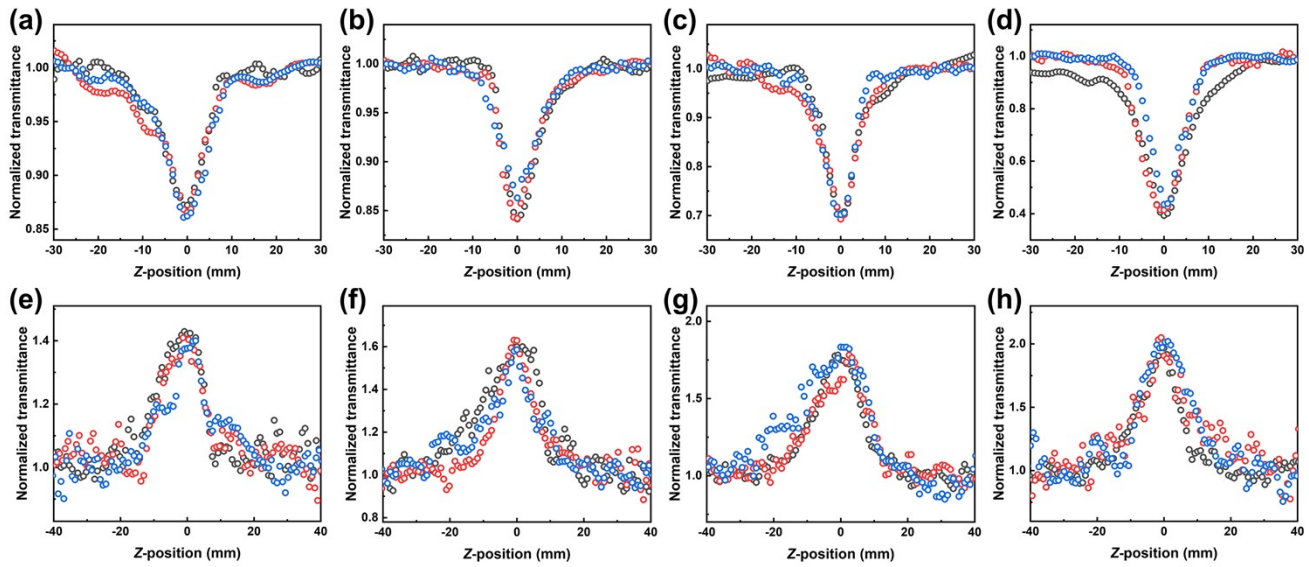

Figure S9. Open-aperture Z-scan curves measured at different positions of the pristine $CsPbBr_3$-NC, ZnPr-$CsPbBr_3$-NC, 0.25 PyMA-$CsPbBr_3$-NC, and ZnPr-0.25 PyMA-$CsPbBr_3$-NC PMMA films under input laser irradiation at (a-d) 800 nm and (e-h) 515 nm.

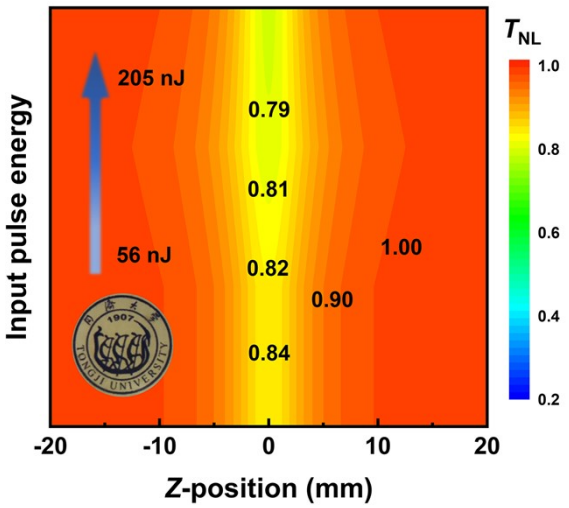

Figure S10. Normalized transmittance distributions of the ZnPr-$CsPbBr_3$-NC PMMA film under input laser irradiation at 800 nm. The image embedded in the lower-left corner is its photograph.

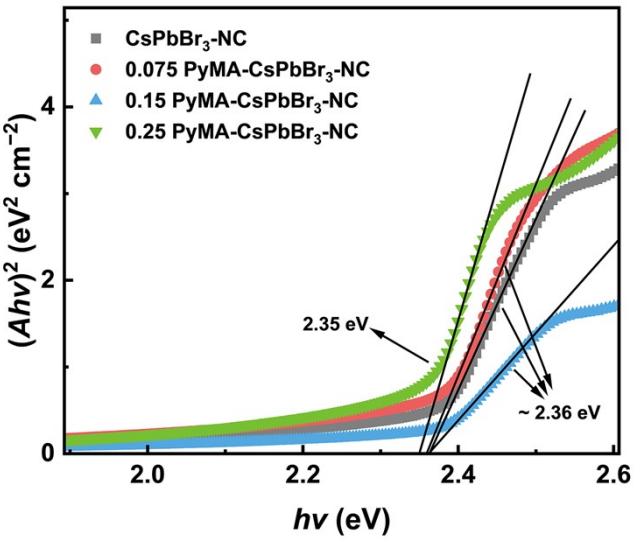

Figure S11. Tauc diagrams for the pristine $CsPbBr_3$-NC and PyMA-modified $CsPbBr_3$-NCs.

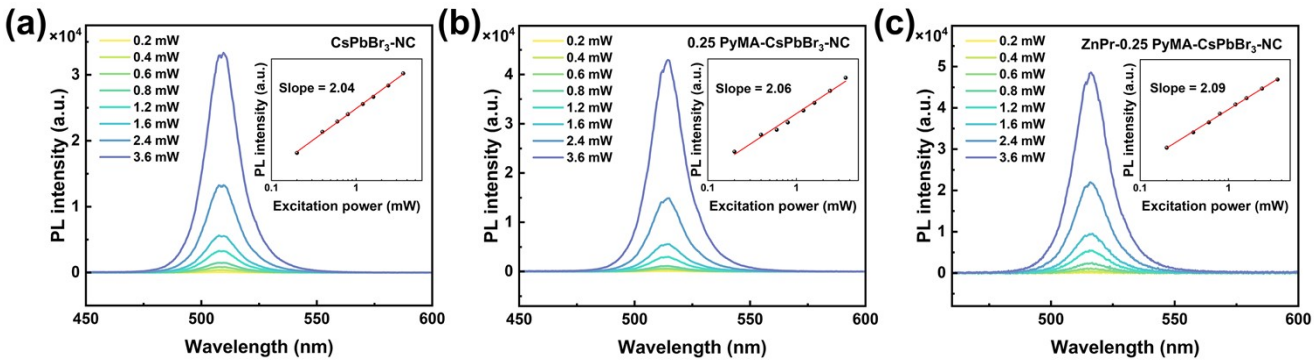

Figure S12. Excitation power-dependent two-photon PL spectra for (a) the pristine $CsPbBr_3$-NC, (b) 0.25 PyMA-$CsPbBr_3$-NC, and (c) ZnPr-0.25 PyMA-$CsPbBr_3$-NC at 800 nm. The corresponding insets show the relationships between the two-photon PL intensity and laser excitation power (log~log).

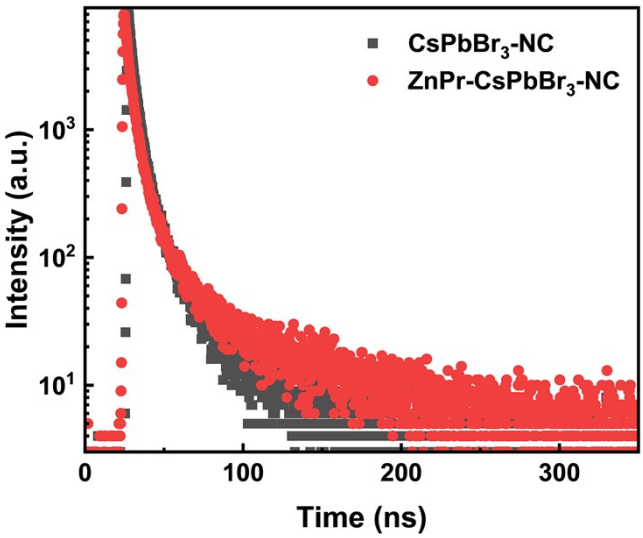

Figure S13. TRPL spectra for the pristine $CsPbBr_3$-NC and ZnPr-$CsPbBr_3$-NC.

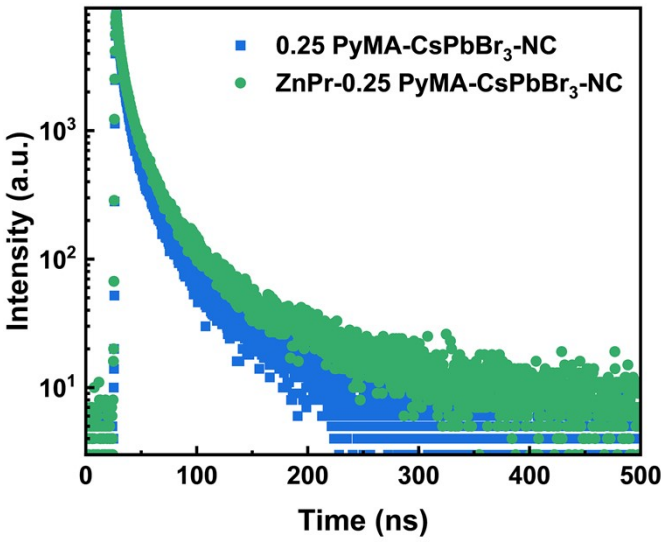

Figure S14. TRPL spectra for the 0.25 PyMA-$CsPbBr_3$-NC and ZnPr-0.25 PyMA-$CsPbBr_3$-NC

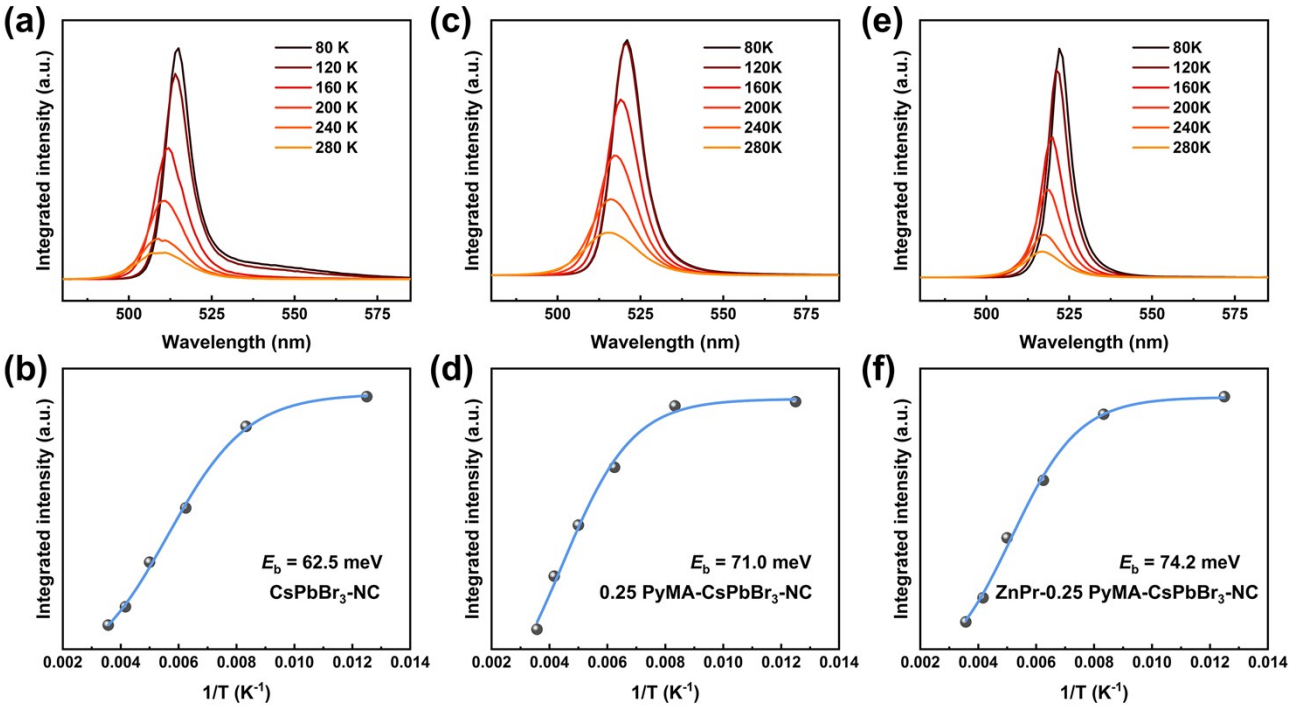

Figure S15. Temperature-dependent PL spectra and corresponding fitting curves (based on the Arrhenius equation) of (a,b) the pristine $CsPbBr_3$-NC, (c,d) 0.25 PyMA-$CsPbBr_3$-NC , and (e,f) ZnPr-0.25 PyMA-$CsPbBr_3$-NC.

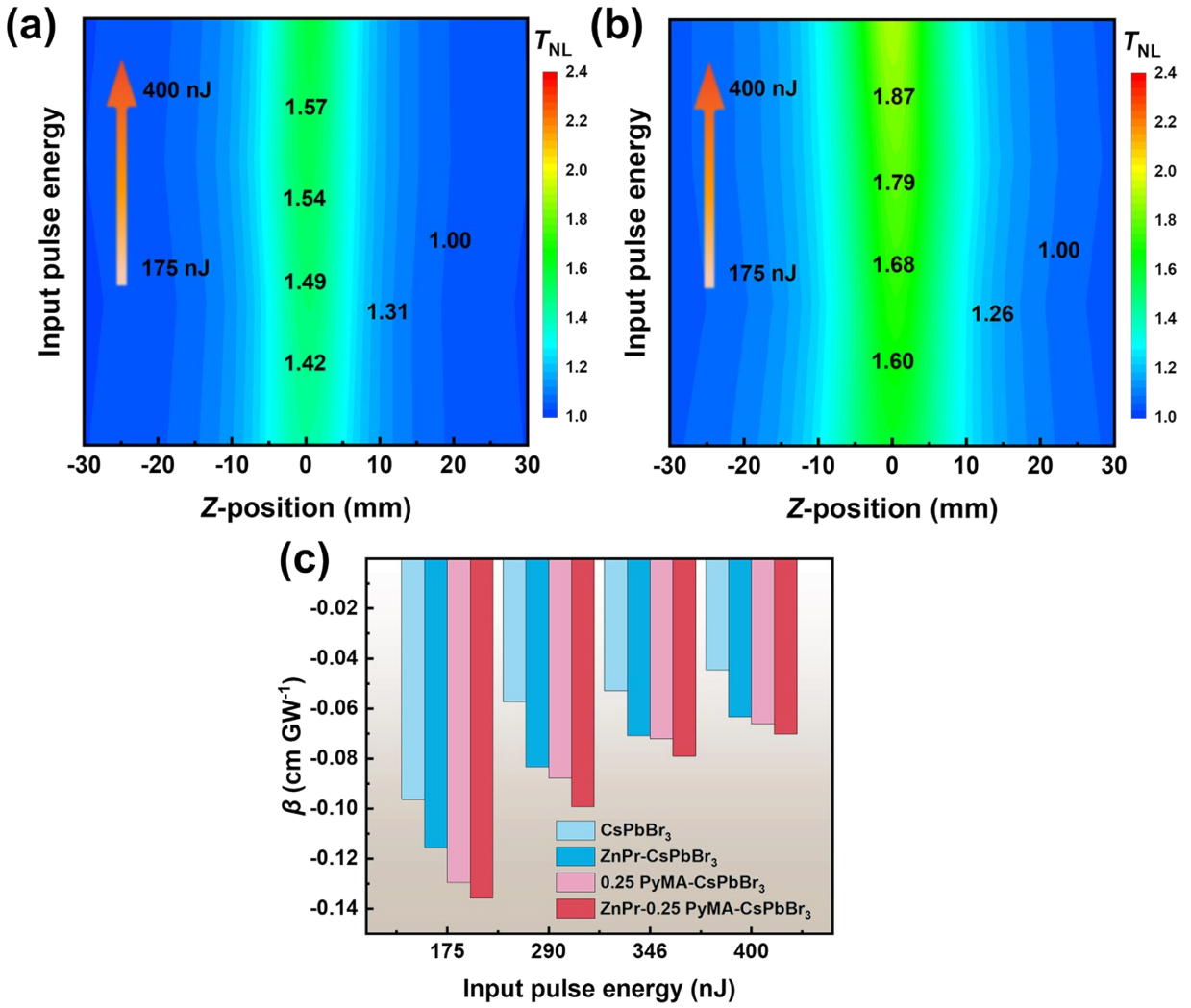

Figure S16. Normalized transmittance distributions of (a) the pristine $CsPbBr_3$-NC and (b) ZnPr-$CsPbBr_3$-NC PMMA film under input laser irradiation at 515 nm. (c) The corresponding β values for all samples.

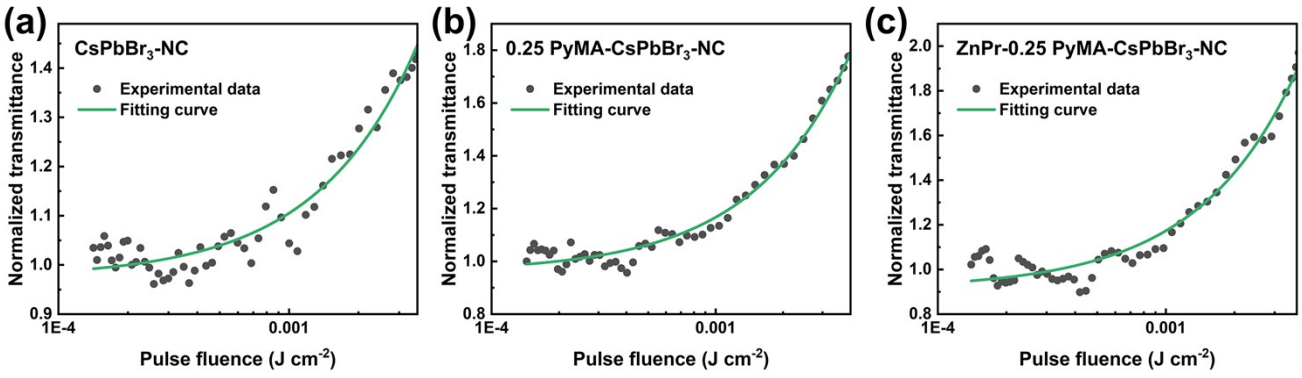

Figure S17. Pulse fluence-dependent normalized transmittance of (a) the pristine $CsPbBr_3$-NC, (b) 0.25 PyMA-$CsPbBr_3$-NC, and (c) ZnPr-0.25 PyMA-$CsPbBr_3$-NC at 515 nm.

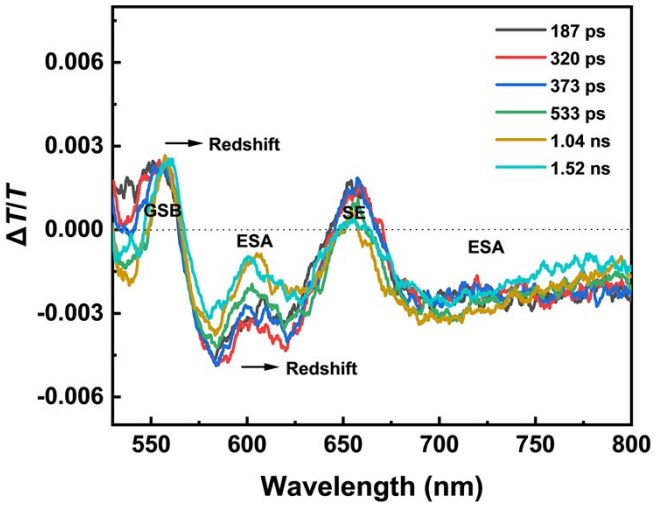

Figure S18. TA spectra for the ZnPr-0.25 PyMA-$CsPbBr_3$-NC at different delay times under 520 nm fs laser pulse excitation.

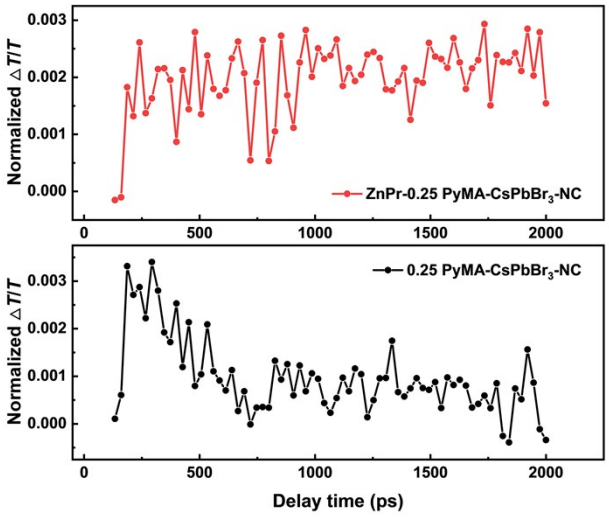

Figure S19. Comparison of bleach recovery kinetics of 0.25 PyMA-$CsPbBr_3$ (bottom) and ZnPr-0.25 PyMA-$CsPbBr_3$ NCs (top) after exciting the samples at 520 nm. The kinetics were monitored at ~556 nm.

Table S1. NLO absorption parameters for all perovskite samples under fs laser excitation at 800 nm with various input pulse energies.

Samples	Laser pulse length	L (μm)	E_I (nJ)[a]	T_{min}	β (cm GW^{-1})
$CsPbBr_3$-NC	34 fs	296	56	0.87	117.52×10^{-3}
			78	0.86	88.16×10^{-3}
			146	0.84	52.50×10^{-3}
			205	0.82	35.62×10^{-3}
ZnPr-$CsPbBr_3$-NC		313	56	0.84	119.98×10^{-3}
			78	0.82	95.95×10^{-3}
			146	0.81	66.82×10^{-3}
			205	0.79	39.13×10^{-3}
0.25 PyMA-$CsPbBr_3$-NC		367	56	0.70	231.99×10^{-3}
			78	0.68	220.69×10^{-3}
			146	0.63	135.70×10^{-3}
			205	0.60	110.54×10^{-3}
ZnPr-0.25 PyMA-$CsPbBr_3$-NC		325	56	0.37	1150.47×10^{-3}
			78	0.35	882.13×10^{-3}
			146	0.32	537.35×10^{-3}
			205	0.28	473.88×10^{-3}

[a]E_I: input pulse energy.

Table S2. NLO absorption parameters for all perovskite samples under fs laser excitation at 515 nm with various input pulse energies.

Samples	Laser pulse length	L (μm)	E_I (nJ)	T_{max}	β (cm GW^{-1})
$CsPbBr_3$-NC	34 fs	296	175	1.43	-96.42×10^{-3}
			290	1.49	-57.22×10^{-3}
			346	1.54	-52.89×10^{-3}
			400	1.57	-44.66×10^{-3}
ZnPr-$CsPbBr_3$-NC		313	175	1.60	-115.64×10^{-3}
			290	1.68	-83.33×10^{-3}
			346	1.79	-70.77×10^{-3}
			400	1.87	-63.39×10^{-3}
0.25 PyMA-$CsPbBr_3$-NC		367	175	1.79	-129.58×10^{-3}
			290	1.95	-87.85×10^{-3}
			346	2.09	-72.13×10^{-3}
			400	2.23	-66.14×10^{-3}
ZnPr-0.25 PyMA-$CsPbBr_3$-NC		325	175	1.96	-135.81×10^{-3}
			290	2.09	-99.29×10^{-3}
			346	2.16	-79.10×10^{-3}
			400	2.33	-70.17×10^{-3}

Table S3. The σ_g and σ_e values of perovskite NCs samples under SA by nonlinear fitting using the Frantz-Nodvik model.

Samples	T_0[a]	N[b] (cm^{-3})	σ_g[c] (cm^2)	σ_e[d] (cm^2)	σ_e/σ_g
$CsPbBr_3$-NC	0.85	2.34×10^{21}	2.33×10^{-21}	1.42×10^{-21}	0.61
0.25 PyMA-$CsPbBr_3$-NC	0.49	2.34×10^{21}	8.31×10^{-21}	3.49×10^{-21}	0.42
ZnPr-0.25 PyMA-$CsPbBr_3$-NC	0.69	2.34×10^{21}	4.84×10^{-21}	1.69×10^{-21}	0.35

[a]T_0: linear transmittance, [b]N: absorber density, [c]σ_g: GSA cross section, [d]σ_e: ESA cross section.

References

1. Y. Mugnier and E. Laviron, *J. Chem. Soc., Perkin Trans. 2*, *1979, 1264-1266.*
2. Q. Tan, H. Chen, H. Xia, B. Liu and B. Xu, *Chem. Commun.*, 2016, **52**, 537-540.
3. C. R. Greaves, M. Á. Alemán García and N. Bampos, *Chem. Commun.*, 2015, **51**, 15689-15691.
4. M. J. Plater, S. Aiken and G. Bourhill, *Tetrahedron*, 2002, **58**, 2405-2413.
5. J. Li, *Name reactions: A collection of detailed mechanisms and synthetic applications: Fourth expanded edition*, 2009.
6. J. Huang, N. Dong, S. Zhang, Z. Sun, W. Zhang and J. Wang, *ACS Photonics*, 2017, **4**, 3063-3070.
7. S. Zhang, Y. Li, X. Zhang, N. Dong, K. Wang, D. Hanlon, J. N. Coleman, L. Zhang and J. Wang, *Nanoscale*, 2016, **8**, 17374-17382.
8. H. Chen, L. Gao, O. A. Al-Hartomy, F. Zhang, A. Al-Ghamdi, J. Guo, Y. Song, Z. Wang, H. Algarni, C. Wang, S. Wageh, S. Xu and H. Zhang, *Nanoscale*, 2021, **13**, 15891-15898.